Communication Resources Allocation for Time Delay Reduction of Frequency Regulation Service in High Renewable Penetrated Power System

Hongjie He, *Student Member*, *IEEE*, Ning Zhang, *Senior Member*, *IEEE*, Chongqing Kang, *Fellow*, *IEEE*, Song Ci, *Fellow*, *IEEE*, Fei Teng, *Senior Member*, *IEEE*, and Goran Strbac, *Member*, *IEEE*

***Abstract*—The high renewable penetrated power system has severe frequency regulation problems. Distributed resources can provide frequency regulation services but are limited by communication time delay. This paper proposes a communication resources allocation model to reduce communication time delay in frequency regulation service. Communication device resources and wireless spectrum resources are allocated to distributed resources when they participate in frequency regulation. We reveal impact of communication resources allocation on time delay reduction and frequency regulation performance. Besides, we study communication resources allocation solution in high renewable energy penetrated power systems. We provide a case study based on the HRP-38 system. Results show communication time delay decreases distributed resources' ability to provide frequency regulation service. On the other hand, allocating more communication resources to distributed resources' communication services improves their frequency regulation performance. For power systems with renewable energy penetration above 70%, required communications resources are about five times as many as 30% renewable energy penetrated power systems to keep frequency performance the same.**

***Index Terms*—Communication resources allocation, communication time delay, distributed resource, frequency regulation, high renewable energy penetrated power system.**

NOMENCLATURE

A. Abbreviation

AGC	Automatic Generation Control.
BAAL	Balancing Authority ACE Limit.
BS	Base Station.
CPS-1	Control Performance Standard 1.
SFC	Service function chain.
VRE	Variable renewable energy.
DVRE	Distributed variable renewable energy.

B. Decision Variables

$X(n^S, n^I)$	Binary variable indicating the infrastructure node n^I is allocated to service node n^S.
$X(e^S, e^I)$	Binary variable indicating the infrastructure link e^I is allocated to service link e^S.
$C_{\text{sys}}^{\text{AL}}$	Communication allocating cost for all SFCs.

C. Parameters

e^I	Infrastructure network link e^I.
n^I	Infrastructure network node n^I.
e^S	SFC's service link e^S.
n^S	SFC's service node n^S.
$c_1(e_{\text{r,b}}^S)$	Radio access spectrum resources requirement of a SFC.
$c_1(n_{\text{b}}^S)$	Bases stations devices resources requirement of a SFC.
$c_1(e_{\text{b,g}}^S)$	Backhaul link spectrum resources requirement of a SFC.
$c_1(n_{\text{g}}^S)$	Gateway devices resources requirement of a SFC.
T_{AGC}	End-to-end time delay of the AGC signals delivering.
T_{bh}	Time delay in the backhaul network.
T_{con}	Time delay of control plane.
T_{ra}	Time delay in the radio access network.
T_{tc}	Time delay in the transmission and core networks.
T_{user}	Time delay of user plane.

I. INTRODUCTION

ACCORDING to International Renewable Energy Agency (IREA), variable renewable energy (VRE) penetration of power system is expected to be 86% in 2050 [1]. VRE is used to denote photovoltaics (PV) and wind turbines. The VRE penetration is electrical energy generated by VRE resources in a given period, divided by the demand of the power system in this period. However, high VRE penetration brings the power system severe frequency regulation problems, which causes the lack of traditional frequency regulation resources and low inertia in the power system [2]. High VRE penetrated power system needs alternative frequency regulation resources urgently. Distributed resources, as emerging technologies, have received significant attention in the AGC due to the reduced greenhouse gas and transmission distance issues [3]. Among these distributed resources, the distributed VRE (DVRE), such

Manuscript received September 15, 2023; accepted October 26, 2023. Date of online publication December 28, 2023; date of current version January 23, 2024. This work was supported in part by the National Key R&D Program of China (No. 2021YFB2401200) and the National Natural Science Foundation of China Enterprise Innovation and Development Joint Fund (No. U21B2002).

H. J. He, N. Zhang (corresponding author, email: ningzhang@tsinghua.edu.cn), C. Q. Kang, and S. Ci are with the State Key Laboratory of Power Systems, Department of Electrical Engineering, Tsinghua University, Beijing 100084, China.

F. Teng and G. Strbac are with the Department of Electrical and Electronic Engineering, Imperial College London, SW7 2BU, London, U.K.

DOI: 10.17775/CSEEJPES.2023.07630

as distributed wind turbines and distributed PV, is a promising frequency regulation resource with its rapid development [4]. However, these DVREs may be in remote and dispersed areas. DVREs need advanced communication technology and enough communication resources to support their participation in frequency regulation.

There have been some researches about frequency regulation services applying advanced communication technology. Distributed resources will rely on 5G to provide a highly responsive, robust, and scalable monitoring and control solution [5]. Research on the potential of using 5G technologies to enable distributed resources in frequency regulation shows that precise load control, ubiquitous data acquisition, and network security are critical in application [6]. A 5G-based fog and cloud computing method is proposed in [7] to help electric vehicles (EVs) provide ancillary services for the power system. A communication network architecture is presented in [8], which can dispatch EVs' charging and discharging behavior to regulate frequency.

Attention has been paid to communication time delay of transmitting a specific service because time delay is the basis for service's performance. A Markov-modulated system is proposed in [9] to analyze end-to-end delay in a communication network for various smart grid applications. An analytical model to evaluate end-to-end delay is established in [10], effectively solving delay-aware virtual network function chain embedding problem. Average delay of a packet transmitting through a switch is analyzed in [11] to support 5G service verticals. Communication delay among distributed generators and dispatch centers is modeled in [12] to study its impact on microgrid's stability and the cost of power management.

There are some experimental researches about time delay in frequency regulation service. Time delay of flexible load providing frequency regulation service is tested in a platform in [13]. Experiments show time delay could be several seconds under some conditions. The impact of time delay on frequency regulation service has been experimented in [14]. Results show time delay significantly deteriorates frequency performance. Experiments in [15] show time delay should be considered when commercial buildings provides frequency regulation service.

Communication resources allocation has been a relevant issue with explosive growth of communication services. A joint edge and central communication resources allocation framework is proposed in [16], which provides an effective means of assigning resources to communication services while meeting their time delay requirements. A communication resources allocation mechanism is proposed in [17], which considers time delay constraints and models resources allocation problem as a mixed integer nonlinear programming problem (MINLP). The user-aware limited communication resource allocation method is proposed in [18], improving energy efficiency while considering users' acceptable maximum delay. A deep learning-based method is proposed in [19] to solve vehicular network's wireless communication resources allocation problems.

The literature review shows communication time delay of DVRE participating in frequency regulation cannot be neglected and may deteriorate frequency regulation performance. Besides, optimizing communication resources allocation can assign resources to communication services and reduce services' time delay. However, these researches have not touched on communication resources allocation for time delay reduction of frequency regulation service.

To fill this gap, we propose a communication resources allocation method to reduce the communication time delay of DVRE participating in frequency regulation. This method allocates wireless spectrum and communication device resources to frequency regulation services while considering services' capacity and delay requirements. Therefore, DVRE can provide frequency regulation service for the high VRE penetrated power system. The contributions of this paper lie in three fields:

- Modeling the relationship between communication resources and time delay of power system frequency regulation service.
- Proposing a communication resources allocation model to reduce time delay in DVRE participating in frequency regulation.
- Analyzing the impact of communication resources allocation on frequency regulation in the high VRE penetrated power system.

The remainder of the paper is organized as follows. Section II models the communication system and its corresponding time delay. Section III states the communication resources allocation problem. Section IV models the communication resources allocation problem. Section V provides the power system's frequency regulation system considering time delay. Section VI carries out a case study based on the HRP-38 system. Finally, conclusions are drawn in Section VII.

II. Communication System Model

A. Overview

In our study, we apply a three-layer communication system consisting of a core network, a transmission network, a backhaul network, and a radio access network. The communication system includes frequency regulation resources, base stations (BSs), hubs, and gateways, as shown in Fig. 1. The thermal generator, the gas turbine, and the hydro generator are directly connected to the upper network. Because these resources are centralized and can communicate with the automatic generation control (AGC) dispatch center in a high-speed way. Some distributed resources communicate with upper network by wireless communication, such as distributed energy storage (ES) and the DVRE. The above six kinds of resources are frequency regulation resources in our study: thermal generator, gas turbine, hydro generator, distributed wind turbine, distributed PV, and distributed ES. With rapid development of 5G technologies, we assume cognitive radio (CR) is applied in radio access network and 5G backhaul technology is applied in backhaul network.

End-to-end time delay of the AGC signal's delivery, denoted as T_{AGC}, is sum of time delay in transmission and core network T_{tc}, backhaul network T_{bh}, and radio access network T_{ra} as follows:

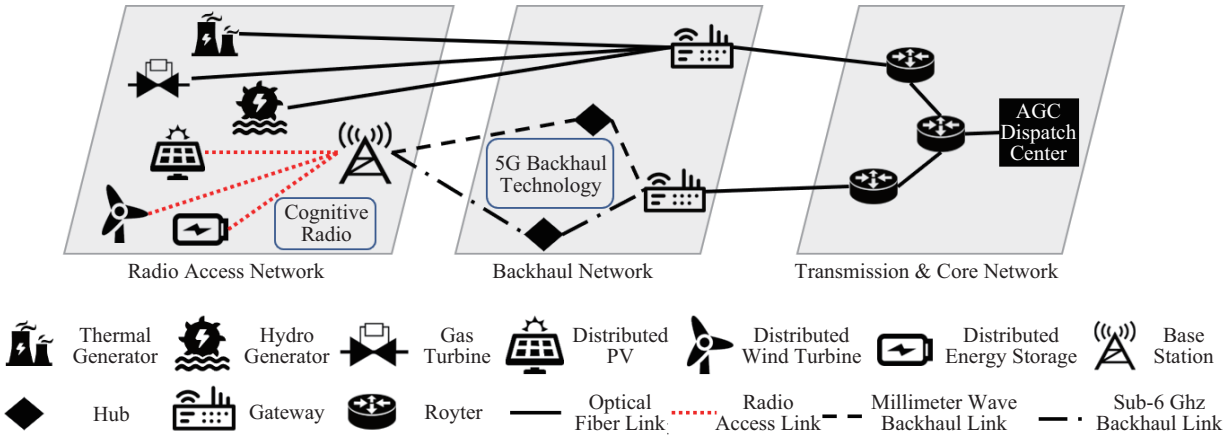

Fig. 1. A communication system model with a radio access network using cognitive radio, a backhaul network using 5G backhaul technology, and a transmission and core network.

$$T_{\mathrm{AGC}} = T_{\mathrm{tc}} + T_{\mathrm{bh}} + T_{\mathrm{ra}} \tag{1}$$

As is studied in [20], time delay in transmission and core network is relatively invariant, which is about 30 milliseconds. Time delay in this network level is negligible compared to time interval of the AGC signal. Therefore, we consider T_{tc} a constant.

B. Time Delay in Radio Access Network

In radio access network, time delay T_{ra} consists of two parts. First part is delay BS allocates an idle channel to user, which is control plane delay, denoted as T_{con}. Second part is delay in BS delivers data to user through channel, which is user plane delay, denoted as T_{user}. Then, we have the following:

$$T_{\mathrm{ra}} = T_{\mathrm{user}} + T_{\mathrm{con}} \tag{2}$$

T_{user} is usually about one millisecond in 5G era, according to International Telecommunication Union (ITU) [21]. However, T_{con} is considerably large due to radio access spectrum resources shortage caused by massive distributed resources accessing channels to BSs. Therefore, we assume CR technology is used in radio access network. CR technology is a spectrum-sharing technology increasing spectrum's utilization by assigning different priorities to channel users. Distributed frequency regulation resources in CR technology will be divided into primary users (PUs) and secondary users (SUs). PUs have priority over SUs in using channels, and SUs share idle channels when PUs are absent from channels. In our study, distributed ES are PUs because they are full-featured in providing frequency regulation service, and we choose the DVRE as SUs. Therefore, ES does not experience T_{con} because of its priority in using channels.

SUs' control plane time delay $T_{\mathrm{con}}^{\mathrm{SU}}$ could be formulated as absorbing time of absorbing Markov process [22]:

$$T_{\mathrm{con}}^{\mathrm{SU}} = l_{\mathrm{ra}} \sum_{m=0}^{M_1} P_{\mathrm{m}} n_{\mathrm{ma}} \tag{3}$$

where l_{ra} is time slot length in radio access network, P_{m} is probability of system beginning from state m, m is the state when there are m out of M_1 channels that are idle, n_{ma} is number of steps transferring from state m to absorbing state.

C. Time Delay in Backhaul Network

Backhaul network mainly consists of links connecting BSs with backhaul gateways that deliver BSs' traffic. Optical fiber backhaul, Sub-6 GHz backhaul, and millimeter backhaul technologies are applied in backhaul network.

Backhaul time delay of the optical fiber backhaul technology $T_{\mathrm{bh}}^{\mathrm{wd}}$ mainly comes from nodes' processing time delay, which could be modeled as the sum of a backhaul gateway's processing delay and $n_{\mathrm{h}} - 1$ hubs' processing delays [23]:

$$T_{\mathrm{bh}}^{\mathrm{wd}} = \left(\left(1 + 1.28 \frac{d_1^{\mathrm{b}}}{d_1^{\mathrm{g}}} \right) \beta_1 + (n_{\mathrm{h}} - 1)\beta_2 \right) (a + b\mu) \tag{4}$$

where d_1^{b} and d_1^{g} are the density of the base station and backhaul gateway in the network, β_1, β_2, a, and μ are processing parameter of gateway and hub, b is the packet size.

Backhaul time delay of the wireless backhaul technology mainly comes from packet transmission. Backhaul time delay is mainly calculated by probability of backhaul gateway serving the base station and probability of successful transmission from the backhaul gateway to base station. The expression is as follows:

$$T_{\mathrm{bh}}^{\mathrm{wl}} = l_{\mathrm{bh}}^{\mathrm{wl}} \frac{1}{P_{\mathrm{gb}} P_{\mathrm{st}}} \tag{5}$$

where $T_{\mathrm{bh}}^{\mathrm{wl}}$ is backhaul time delay of the wireless backhaul technology, $l_{\mathrm{bh}}^{\mathrm{wl}}$ is the time slot length of the wireless backhaul technology, P_{gb} is probability of a backhaul gateway serving a specific base station, P_{st} is probability of a single successful transmission.

We assume the backhaul gateway serves all connected base stations with equal probability, then probability that a backhaul gateway serves a particular base station is inverse of the average number of base stations connected to the gateway:

$$P_{\mathrm{gb}} = \frac{1}{1 + 1.28 \frac{d_1^{\mathrm{b}}}{d_1^{\mathrm{g}}}} \tag{6}$$

For Sub-6 GHz wireless backhaul technology, single successful transmission probability $P_{\mathrm{st}}^{\mathrm{s6}}$ is [24]:

$$P_{\mathrm{st}}^{\mathrm{s6}} = \frac{1}{1 + D(\alpha, \theta)} \tag{7}$$

where $D(\alpha,\theta) = \theta^{\frac{2}{\alpha}} \int_{\theta^{-\frac{2}{\alpha}}}^{\infty} \frac{1}{1+u^{\frac{\alpha}{2}}} \mathrm{d}u$, θ is the threshold of received signal-to-interference, α is the path loss exponent.

For millimeter wave wireless backhaul technology, single successful transmission probability $P_{\mathrm{st}}^{\mathrm{mm}}$ is:

$$P_{\mathrm{st}}^{\mathrm{mm}} = \boldsymbol{P}(L \leqslant \pi_{\mathrm{tx}} - \theta - N_0 B_{\mathrm{bh}}^{\mathrm{mm}}) \tag{8}$$

where $\boldsymbol{P}(\cdot)$ is probability expression, π_{tx} is transmit power plus antenna gains in dBm, N_0 is noise power density, $B_{\mathrm{bh}}^{\mathrm{mm}}$ is bandwidth of millimeter wave backhaul links, L is path loss of a stadia link with distance r [25]:

$$L(\mathrm{dB}) = 70 + 20\log_{10}(r) + \xi,\ \xi \sim \mathcal{N}(0,\sigma^2) \tag{9}$$

where ξ is the shadow fading coefficient, σ is the standard deviation of shadow fading in dB, $\mathcal{N}(\cdot)$ is a normal distribution.

According to (8) and (9), we can have:

$$\begin{aligned} P_{\mathrm{st}}^{\mathrm{mm}} &= \boldsymbol{P}(\xi \leq \pi_{\mathrm{tx}} - \theta - N_0 B_{\mathrm{bh}}^{\mathrm{mm}} - 70 - 20\log_{10}(r)) \\ &= \frac{1}{2}\left(1 + \mathrm{erf}\left(\frac{\theta'(r)}{\sqrt{2}\sigma}\right)\right) \end{aligned} \tag{10}$$

where $\mathrm{erf}(\cdot)$ is the error function, $\theta'(r) = \pi_{\mathrm{tx}} - \theta - N_0 B_{\mathrm{bh}}^{\mathrm{mm}} - 70 - 20\log_{10}(r)$. Therefore, delay of each hop in millimeter wave backhaul link is $1/(P_{\mathrm{st}}^{\mathrm{mm}} P_{\mathrm{gb}})$, and backhaul time delay of millimeter wave can be obtained by multiplying hop number n_h and time slot length.

According to (5) to (10), Sub-6 GHz backhaul links time delay $T_{\mathrm{bh}}^{\mathrm{s6}}$ and millimeter wave backhaul links time delay $T_{\mathrm{bh}}^{\mathrm{mm}}$ as follows:

$$T_{\mathrm{bh}}^{\mathrm{s6}} = l_{\mathrm{bh}}^{\mathrm{s6}} \left(1 + 1.28\frac{d_1^{\mathrm{b}}}{d_1^{\mathrm{g}}}\right)(1 + D(\alpha,\theta)) \tag{11}$$

$$T_{\mathrm{bh}}^{\mathrm{mm}} = l_{\mathrm{bh}}^{\mathrm{mm}} \left(1 + 1.28\frac{d_1^{\mathrm{b}}}{d_1^{\mathrm{g}}}\right) \frac{2n_{\mathrm{h}}}{\left(1 + \mathrm{erf}\left(\frac{\theta'(r)}{\sqrt{2}\sigma}\right)\right)} \tag{12}$$

Table I provides the composition of AGC end-to-end time delay in different frequency regulation resources. $T_{\mathrm{AGC}}^{\mathrm{Th}}$, $T_{\mathrm{AGC}}^{\mathrm{G}}$, $T_{\mathrm{AGC}}^{\mathrm{H}}$, $T_{\mathrm{AGC}}^{\mathrm{ES}}$, $T_{\mathrm{AGC}}^{\mathrm{W}}$, and $T_{\mathrm{AGC}}^{\mathrm{PV}}$ is the AGC end-to-end time delay in thermal generator, gas turbine, hydro generator, distributed ES, distributed wind turbines, and distributed PV, respectively.

TABLE I
COMPOSITION OF AGC END-TO-END TIME DELAY IN DIFFERENT FREQUENCY REGULATION RESOURCES

Delay Type (ms)	$T_{\mathrm{AGC}}^{\mathrm{Th}}$	$T_{\mathrm{AGC}}^{\mathrm{G}}$	$T_{\mathrm{AGC}}^{\mathrm{H}}$	$T_{\mathrm{AGC}}^{\mathrm{ES}}$	$T_{\mathrm{AGC}}^{\mathrm{W}}$	$T_{\mathrm{AGC}}^{\mathrm{PV}}$
Control Plane T_{con}	–	–	–	–	✓	✓
User Plane T_{user}	–	–	–	✓	✓	✓
Backhaul T_{bh}	–	–	–	✓	✓	✓
Transmission & Core Network T_{tc}	✓	✓	✓	✓	✓	✓

III. COMMUNICATION RESOURCES ALLOCATION PROBLEM STATEMENT

A. Overview

Figure 2 presents three main layers in communication resources allocation problem: infrastructure layer, communication service layer, and allocating layer. In the infrastructure layer, infrastructure network possesses physical communication resources, such as communication devices, access spectrum resources, and backhaul spectrum resources. In 5G era, communication resources are not specified for a specific service but can be shared and allocated to different communication services. In the service layer, communication service is modeled as a service function chain (SFC) with service nodes and connecting service links. Each service node represents communication service's function at each communication network level. Each service link represents service's communication link between different network levels. Service nodes and service links have capacity requirements for communication resources to support communication service. In the allocating layer, infrastructure network allocates communication resources to an SFC considering SFC's capacity requirements, time delay requirements, and allocating cost.

B. Infrastructure Network

In our study, we model infrastructure communication network as a weighted undirected graph and denote it by $G^I = (N^I, E^I)$, where N^I is the set of infrastructure network nodes, and E^I is the set of infrastructure network links. Each infrastructure network node n^I in N^I has three attributes, which are node resources' maximum capacity limit $\bar{c}(n^I)$, node resources' capacity price $p(n^I)$, and geographic location

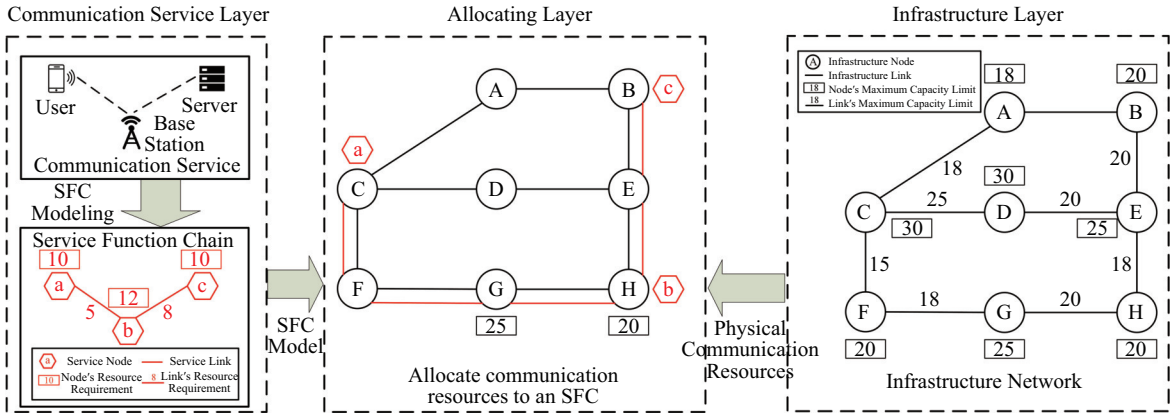

Fig. 2. The communication service layer, allocating layer, and infrastructure layer in the communication resources allocation problem.

$loc(n^I)$. Each infrastructure network link $e^I_{i,j}$ connecting infrastructure network node i and infrastructure network node j has two attributes, which are link resources' maximum capacity $\bar{c}(e^I_{i,j})$ and link resources' capacity price $p(e^I_{i,j})$.

C. Service Function Chain

SFC is a graphical representation of a communication service consisting of service nodes and their connecting service links. As shown in Fig. 2, we model SFCs as weighted undirected graphs and denote an SFC by $G^S = (N^S, E^S)$. Each service node $n^S \in N^S$ and service link $e^S \in E^S$ of an SFC require communication resources to support communication service, whose resources requirements are denoted as $c(n^S)$ and $c(e^S)$. Therefore, the SFC relies on the communication resources in the infrastructure network to carry on the SFC, and infrastructure network will allocate communication resources to the SFC. Each service node has a non-negative attribute value $D(n^S)$ limiting allocating distance. When allocating resources to the SFCs, constraints of the SFCs' resources requirements and locations should be considered.

In our study, an SFC represents frequency regulation communication service transmitted from distributed frequency regulation resources in access network to AGC dispatch center in the core network. As described in Section II, service nodes of frequency regulation communication service consist of four parts: distributed frequency regulation resources, base stations, backhaul gateways, and AGC dispatch center. Therefore, we model frequency regulation service as an SFC consisting of four service nodes and three service links, as shown in Fig. 3. We assume communication resources capacity requirements of the AGC dispatch center's node $c(n^S_{\mathrm{d}})$ and links that connect gateway and AGC dispatch center node $c(e^S_{g,d})$ are fixed. Besides, we assume communication resources capacity requirements of frequency regulation resources' nodes $c(n^S_{\mathrm{r}})$ are fixed. These resources are fixed because allocating more resources to these nodes and links makes no difference to overall time delay.

D. Relationship Between Communication Resources and Time Delay in Frequency Regulation's SFC

In our study, we assume there are two communication resource requirements cases: base communication resources case c_0 and extra allocated communication resources case c_1. In base communication resources case c_0, communication resources allocated to SFCs are base values. But in extra allocated resources case c_1, we allocate extra communication resources to SFCs to show effectiveness of allocating extra communication resources compared to case c_0. Base communication resources case c_0 is benchmark in our study. In case c_1, communication resources requirements of links connecting frequency regulation resources and base stations $c_1(e^S_{\mathrm{r,b}})$, base station nodes $c_1(n^S_{\mathrm{b}})$, links connecting base stations and gateways $c_1(e^S_{\mathrm{b,g}})$, and gateway nodes $c_1(n^S_{\mathrm{g}})$ in an SFC are unfixed and to be allocated. These four communication resources requirements will all vary with frequency regulation service's quality requirement, such as required service communication delay decreasing, leading to required communication resources increasing. But these four communication resources

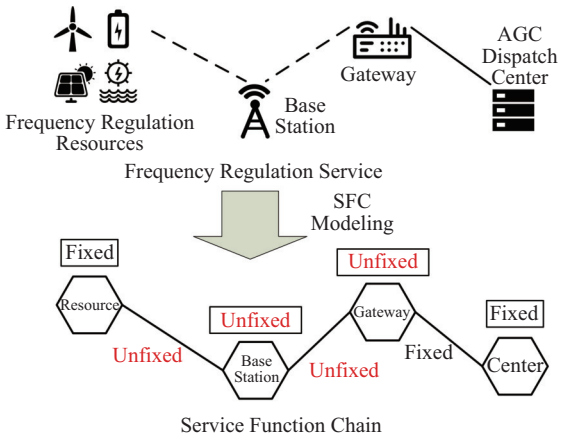

Fig. 3. Modeling the frequency regulation communication service into an SFC.

requirements are independent of each other since each only influences time delay of its own communication network part, for example, gateway nodes resources only affect data packet's processing delay of gateway, and backhaul links resources only affect data packet's transmission delay. So, there is no relationship between node and link resources requirements. In the following section, we study the relationship between communication resources and time delay of its own communication network part. After doing this, we can allocate wireless spectrum resources and communication device resources to the above four communication resources requirements to change end-to-end time delay of frequency regulation service. Specifically, $c_1(n^S_{\mathrm{b}})$ and $c_1(n^S_{\mathrm{g}})$ determine spatial density of base stations and gateways, which are d^{b}_1 and d^{g}_1 in our study as follows:

$$d^{\mathrm{b}}_1 = \frac{c_1(n^S_{\mathrm{b}})}{c_0(n^S_{\mathrm{b}})} d^{\mathrm{b}}_0 \quad d^{\mathrm{g}}_1 = \frac{c_1(n^S_{\mathrm{g}})}{c_0(n^S_{\mathrm{g}})} d^{\mathrm{g}}_0 \tag{13}$$

where $c_0(n^S_{\mathrm{b}})$ and $c_0(n^S_{\mathrm{g}})$ are base values of nodes' base stations and gateways resources requirements, d^{b}_0 and d^{g}_0 are base values of base stations' and gateways' density.

$c_1(e^S_{\mathrm{r,b}})$ determines radio access spectrum resources, which are linear to the number of radio access channels M_1 in our study as follows:

$$M_1 = \frac{c_1(e^S_{\mathrm{r,b}})}{c_0(e^S_{\mathrm{r,b}})} M_0 \tag{14}$$

where $c_0(e^S_{\mathrm{r,b}})$ is base value of radio access spectrum resources' requirement, and M_0 is base value of number of radio access channels.

$c_1(e^S_{\mathrm{b,g}})$ determines wireless backhaul link spectrum resources, which is equal to bandwidth of wireless backhaul links W in the Shannon–Hartley theorem:

$$C = W \log_2 (1 + \theta) \tag{15}$$

According to (15), when channel transmission rate C is fixed, bandwidth of wireless backhaul links W affects threshold of received signal-to-interference θ. According to (7) and (8), the threshold of received signal-to-interference θ affects

single successful transmission probability in the wireless backhaul link, which determines backhaul links time delay. In our study, wireless backhaul link spectrum resources $c_1(e^S_{\mathrm{b,g}})$ is equal to the bandwidth of wireless backhaul links W, which is $W = c_1(e^S_{\mathrm{b,g}})$. When we need a fixed channel transmission rate C, we have the following equations for different wireless backhaul link spectrum resources:

$$\begin{aligned} C &= c_0(e^S_{\mathrm{b,g}})\log_2(1+\theta_0) \\ C &= c_1(e^S_{\mathrm{b,g}})\log_2(1+\theta_1) \end{aligned} \tag{16}$$

According to (16), the relationship between $c_1(e^S_{\mathrm{b,g}})$ and θ_1 is as follows:

$$\theta_1 = (1+\theta_0)^{\frac{c_0(e^S_{\mathrm{b,g}})}{c_1(e^S_{\mathrm{b,g}})}} - 1 \tag{17}$$

where $c_0(e^S_{\mathrm{b,g}})$ is the base value of backhaul link spectrum resources' requirement, and θ_0 is the base value of received signal-to-interference.

From (13) to (17), we can get relationships between communication resources requirements and communication parameters, which are spatial density of base stations d_1^{b} and gateways d_1^{g}, number of radio access channels M_1, and received signal-to-interference θ_1. So, communication resources requirements determine communication system parameters and thus affect communication time delay. Communication time delay can be calculated by the proposed model in Section II.

IV. Communication Resources Allocation Model

Communication resources allocation problem is an NP-hard problem, which has two aspects, service node's allocation problem and service link's allocation problem [26]. Many researchers solve these two problems separately to reduce computation complexity. Their proposed models focus primarily on service link's allocation problem after employing greedy methods to solve service node's allocation problem [27]–[29]. Unlike the above models, our proposed communication resources allocation model coordinately considers service node's allocation and service link's allocation by introducing binary variables and binary constraints. Specifically, our model optimizes the SFCs' deployment and allocating cost by considering allocating constraints and SFCs' constraints.

A. Objective Function

The objective function is to minimize allocating cost $C^{\mathrm{AL}}_{\mathrm{sys}}$, including node resources use cost and link resources use cost in allocating infrastructure network's communication resources. Node resources use cost is product of communication resources requirements of all service nodes $\sum_{n^S=1}^{N^S} X(n^S,n^I)c(n^S)$ and corresponding node resources' capacity price $p(n^I)$. The value of $X(n^S,n^I)$ being 1 indicates infrastructure node n^I is allocated to service node n^S. Link resources use cost is product of communication resources requirements of service links $\sum_{e^S=1}^{E^S} X(e^S,e^I)c(e^S)$ and corresponding link resources' capacity price $p(e^I)$. The value of $X(e^S,e^I)$ being 1 indicates infrastructure link e^I is allocated to service link e^S.

$$\begin{aligned} \min\ C^{\mathrm{AL}}_{\mathrm{sys}} = &\sum_{n^I=1}^{N^I} p(n^I) \sum_{n^S=1}^{N^S} X(n^S,n^I)c(n^S) \\ &+ \sum_{e^I=1}^{E^I} p(e^I) \sum_{e^S=1}^{E^S} X(e^S,e^I)c(e^S) \end{aligned} \tag{18}$$

B. Resources Allocation Constraints

1) Capacity Limit Constraints

Equation (19) is infrastructure network resources capacity constraint. Equation (19) ensures any allocated infrastructure node and link must meet its communication resources capacity limit.

$$\begin{aligned} &\sum_{e^S=1}^{E^S} X(e^S,e^I)c(e^S) \le \overline{c}(e^I),\ \forall e^I \in E^I \\ &\sum_{n^S=1}^{N^S} X(n^S,n^I)c(n^S) \le \overline{c}(n^I),\ \forall n^I \in N^I \end{aligned} \tag{19}$$

2) Allocated Node's Distance Constraints

Equation (20) models allocated node's distance constraint. Distance$[i,j]$ denotes the distance between node i and node j. M is the big M value. When infrastructure node n^I is allocated to service node n^S, (20) ensures allocated location $loc(n^I)$ is not more than $D(n^S)$ away from specific allocated location $loc(n^S)$. This constraint helps to allocate nearby communication resources to the service to avoid unacceptably large communication time delays caused by long-distance access [29], [30].

$$\begin{aligned} &\mathrm{Distance}[loc(n^I), loc(n^S)] - D(n^S) \\ &\quad \le (1 - X(n^S,n^I))M,\ \forall n^S \in N^S, \forall n^I \in N^I \end{aligned} \tag{20}$$

3) SFC's Flow Constraints

Equation (21) models communication traffic flow balance in infrastructure network, which keeps the flow entering the node equal to the flow leaving the node. $e^I_{s,t}$ denotes infrastructure link from source node s to end node t.

$$X(e^S, e^I_{s,t})c(e^S) = X(e^S, e^I_{t,s})c(e^S),\ \forall e^S \in E^S \tag{21}$$

4) Allocation Exclusive Constraints

Equation (22) ensures that only one infrastructure link and one infrastructure node will be allocated to a specific service link and a service node.

$$\begin{aligned} &\sum_{e^I=1}^{E^I} X(e^S,e^I) = 1,\ \forall e^S \in E^S \\ &\sum_{n^I=1}^{N^I} X(n^S,n^I) = 1,\ \forall n^S \in N^S \end{aligned} \tag{22}$$

In summary, (18) to (22) compose the communication resources allocation model, which is an integer linear problem (ILP) and can be efficiently solved by off-the-shelf solvers. Communication network's topology, resources parameters of communication network's nodes and links, and SFCs' communication resources requirement are all parameters of our model. Real-time condition in communication network leads

to above parameters being time-varying. Communication network's parameters can be measured by measuring equipment in the network. The SFCs' resources requirement parameters are offered by distributed resources. So these parameters can be obtained and used as input parameters for our model.

V. Power System Frequency Regulation System

Power system's frequency regulation system is shown in Fig. 4. By evaluating frequency regulation performance in this frequency regulation system, we study effectiveness of communication resources allocation on delay reduction of frequency regulation service. Frequency dynamics can be formulated by first-order swing equation as follows:

$$2H\frac{\mathrm{d}\Delta f(t)}{\mathrm{d}t} = \Delta P_{\mathrm{s}}(t) - \Delta P_{\mathrm{af}}(t) - D\Delta f(t) \tag{23}$$

where H and D are power system's inertia constant and load-damping constant, $\Delta f(t)$, $\Delta P_{\mathrm{s}}(t)$, and $\Delta P_{\mathrm{af}}(t)$ are frequency deviation, power system supply deviation, and power system active power fluctuation, respectively.

We assume thermal generator, gas turbine, and hydro generators conduct primary frequency response when active power imbalance accrues. We also assume all six kinds of generators can participate in secondary frequency response. AGC signals are transmitted from AGC dispatch center to resources through communication network, and there is a communication time delay T_{AGC} in AGC signals' transmission.

VI. Case Study

A. Test System Description

In this section, we use the HRP-38 system to show impact of communication resources allocation on end-to-end communication time delay and frequency regulation performance. The HRP-38 system is based on a real power grid in China, whose VRE energy penetration is about 30%. Frequency regulation service in our manuscript is offered by both centralized resources and distributed resources. We assume thermal generators, gas turbines, hydro generators, wind turbines, and PV can provide 4%, 4%, 8%, 1%, and 1% of the installed capacity for AGC. Parameters settings are shown in Table II [31]. Since wind power and solar power are currently mainstream renewable energy generation methods, we choose these two types of generators to participate in AGC frequency regulation. We use parameters in reference [32] to set up generators' frequency response characteristics. Power system's net load fluctuation due to load and VRE generation fluctuation is shown in Fig. 5.

We use parameters in references [21] for the communication system in our study, which is shown in Table III in the Appendix. Node resources' capacity price and link resources' capacity price are all set uniformly distributed to study impact of the infrastructure network on the SFC deployment [29], [33]. The specific price value is offered by the infrastructure resources provider. In our study, we set all prices uniformly distributed between 15 and 25, which can change according

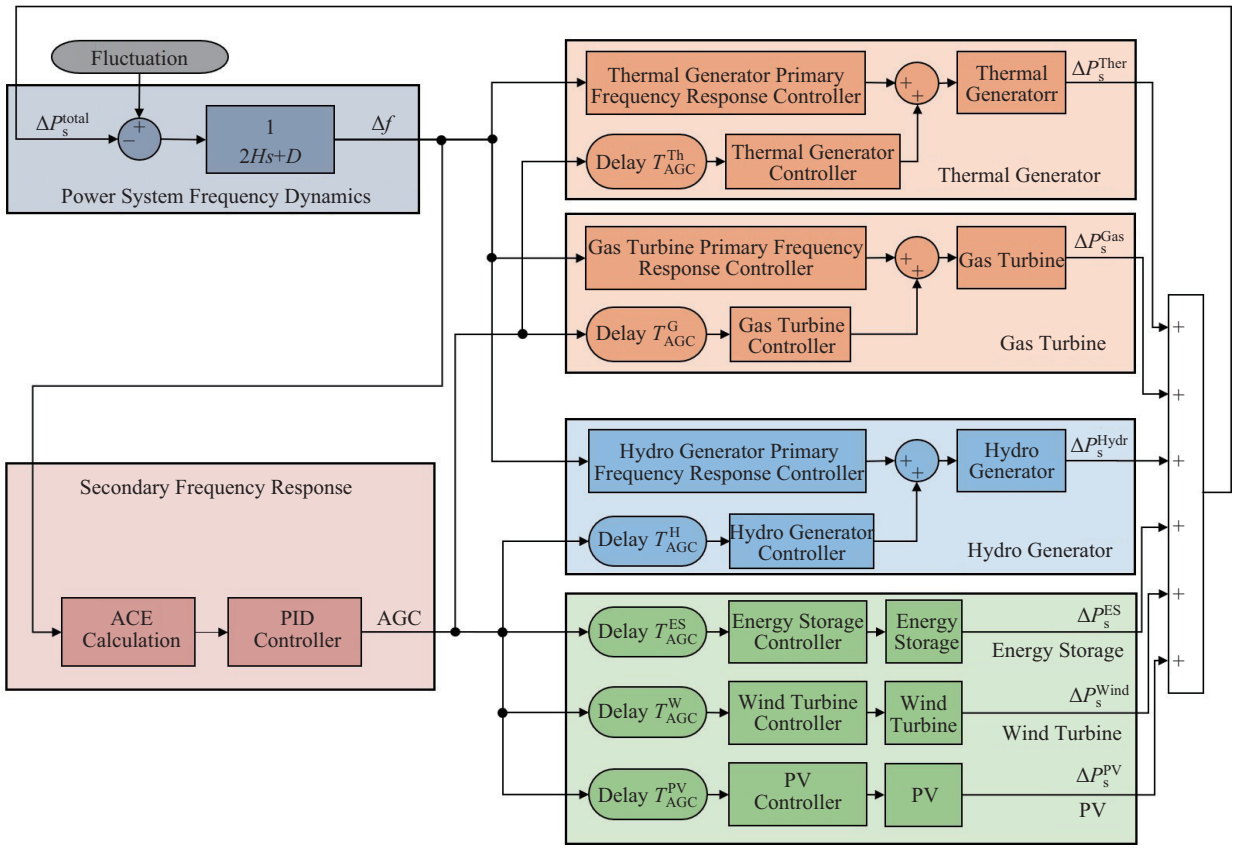

Fig. 4. Frequency regulation system of the power system considering communication time delay.

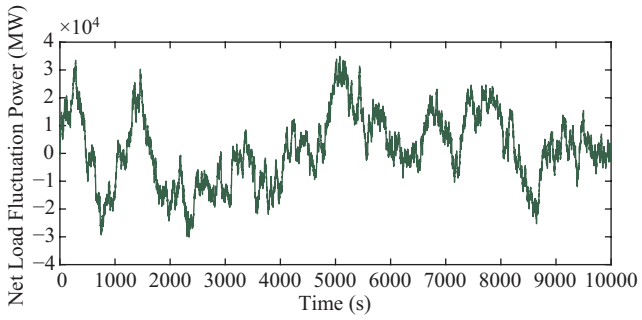

Fig. 5. Power system's net load fluctuation.

TABLE II
PARAMETER SETTINGS OF MAIN POWER SOURCES AND THEIR PARTICIPATING PROPORTION TO AGC IN HRP-38 SYSTEM

Generator Type	Installed Capacity	Proportion to AGC
Thermal Generator	215.6 GW	4%
Gas Turbine	46 GW	4%
Hydro Generator	67 GW	8%
Wind Turbine	110.4 GW	1%
PV	183.9 GW	1%
Peak Load	281.1 GW	–

TABLE III
COMMUNICATION SYSTEM PARAMETER SETTINGS

Parameter	Value	Parameter	Value
α	3.5	β_1	1
β_2	10	μ	0.01 μs/bit
σ	5	θ_0	[0.1, 50]
$l_{\mathrm{bh}}^{\mathrm{mm}}$	125 μs	$l_{\mathrm{bh}}^{\mathrm{s6}}$	500 μs
l_{ra}	143 μs	π_{tx}	30 dBm
d_0^{b}	5×10^{-4}/m^2	d_0^{g}	1×10^{-5}/m^2
N_0	−174 dBm/Hz	l_{mm}	100 m
a	2 μs	b	50 bit
M_0	8	n_{su}	70
$B_{\mathrm{bh}}^{\mathrm{mm}}$	200 MHz	n_{pu}	6
$c_0(e_{\mathrm{r,b}}^S)$	8	$c_0(n_{\mathrm{b}}^S)$	100
$c_0(e_{\mathrm{b,g}}^S)$	100	$c_0(n_{\mathrm{g}}^S)$	10
$p(e_{\mathrm{r,b}}^I)$	[15, 25]	$p(n_{\mathrm{b}}^I)$	[15, 25]
$p(e_{\mathrm{b,g}}^I)$	[15, 25]	$p(n_{\mathrm{g}}^I)$	[15, 25]

to actual situation. We assume distributed ES, wind turbine, and PV connect to BSs through the radio access network, which uses optical fiber, Sub-6 GHz, and millimeter wave technologies in backhaul network. Fig. 6 shows infrastructure network topology of the communication system.

We implement the communication resources allocation model in MATLAB R2019b and solve it by CPLEX. The model includes 11023 constraints and 3874 variables, of which 2595 variables are continuous and 1279 variables are binary. We simulate power system frequency regulation by using MATLAB R2019b and SIMULINK V10.0. Besides, we evaluate frequency performance by control performance standard 1 (CPS-1), balancing authority ACE limit (BAAL), and root mean square error (RMSE) indexes.

B. Results Analysis

1) Impact of Time Delay on AGC

This subsection compares frequency performances in three cases: no DVRE participating in AGC, 1.0% DVRE participating in AGC considering end-to-end time delay T_{AGC}, and 1.0% DVRE participating in AGC without considering end-to-end time delay T_{AGC}. 1.0% DVRE means DVRE's installed capacity is 1% of the peak load of the HRP-38 system. Based on communication time delay model and base communication resources case c_0, we can calculate end-to-end time delay T_{AGC} when DVRE participates in AGC, as shown in Table IV. We can see from Table IV communication time delays in distributed wind turbine and PV are around 1 second. We find using cognitive radio technology in radio access network results in about 471 ms time delay while wired technology has a relatively low time delay. Besides, we find Sub-6 GHz and millimeter wave technologies will have different communication delays though they are all wireless technologies. According to Table IV, wind turbines using Sub-6 GHz technology will have a 417 ms backhaul time delay, and PV using millimeter wave technology will have an 815 ms backhaul time delay. However, ES generator using optical fiber technology will have a 19 ms backhaul time delay. From Table IV, we can see various communication technologies have different communication time delays, and applying different communication technologies will have different impacts on frequency regulation services.

We set time delay in frequency regulation model according to Table IV and perform power system frequency simulation. Frequency regulation performance indexes are shown in Table V. We can see from Table V when there is 1.0% DVRE participating in AGC, the CPS-1 will increase from 89.8%

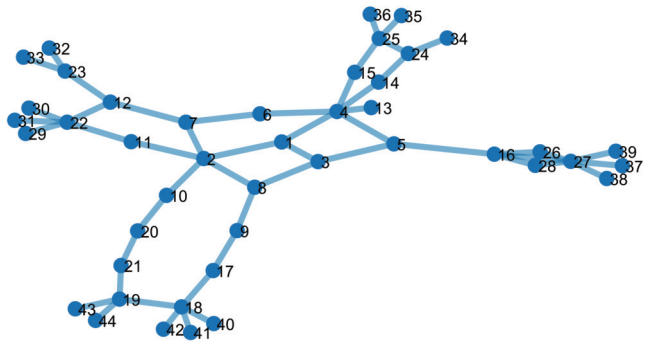

Fig. 6. Infrastructure network topology of the communication system.

TABLE IV
COMMUNICATION TIME DELAY OF DIFFERENT GENERATORS

Delay Type (ms)	$T_{\mathrm{AGC}}^{\mathrm{Th}}$	$T_{\mathrm{AGC}}^{\mathrm{G}}$	$T_{\mathrm{AGC}}^{\mathrm{H}}$	$T_{\mathrm{AGC}}^{\mathrm{ES}}$	$T_{\mathrm{AGC}}^{\mathrm{W}}$	$T_{\mathrm{AGC}}^{\mathrm{PV}}$
Control Plane T_{con}	–	–	–	–	471	471
User Plane T_{user}	–	–	–	1	1	1
Backhaul T_{bh}	–	–	–	19	417	815
Transmission & Core Network T_{tc}	30	30	30	30	30	30
Total T_{AGC}	30	30	30	50	919	1317

TABLE V
FREQUENCY REGULATION PERFORMANCE IN THREE CASES

Case	CPS-1	BAAL	RMSE
No DVRE in AGC	89.8%	99.4%	0.0649
1.0% DVRE in AGC with Delay	91.2%	99.4%	0.0632
Performance Improvement	1.44%	0%	2.62%
1.0% DVRE in AGC without Delay	100.4%	99.4%	0.0561
Performance Improvement	11.80%	0%	13.56%

to 100.4%, and RMSE will decrease from 0.0649 to 0.0561. But when considering communication delay, frequency regulation performance of DVRE will shrink. CPS-1 will decrease from 100.4% to 91.2%, and the RMSE will increase from 0.0561 to 0.0632. Besides, the CPS-1 and RMSE of 1.0% DVRE participating in AGC considering time delay is near to those indexes without DVRE participating in AGC. Simulation results show DVRE can provide frequency regulation support for power system, improving power system frequency performance. However, communication time delay prevents the DVRE from achieving its 100% ability. When time delay is around 1 second, DVRE can barely provide frequency regulation service. Therefore, allocating more communication resources to reduce time delay helps DVRE participate in AGC.

2) Impact of Communication Resources on Time Delay

In this subsection, we study the impact of four communication resources, which are $c_1(e^S_{\mathrm{r,b}})$, $c_1(n^S_{\mathrm{b}})$, $c_1(e^S_{\mathrm{b,g}})$, and $c_1(n^S_{\mathrm{g}})$, on end-to-end communication time delay, respectively. Millimeter wave and Sub-6 GHz technology are two wireless backhaul technologies used in our proposed communication system. So, we carry out our case study by considering these two wireless backhaul technologies separately to calculate end-to-end communication time delay. So, we study impact of communication resources on end-to-end delay when system applies different backhaul technologies. The relationship between communication resources and communication time delay is shown in Fig. 7. As shown in Fig. 7(a), end-to-end time delay experiences a fast decrease first and increases with increase of base station resources. Therefore, allocating more base station resources to frequency regulation's SFC will increase time delay instead of decreasing it. This is because probability gateway serves each base station decreases when there are more base station device resources. End-to-end time delay decreases with increase of gateway device resources, backhaul link spectrum resources, and the number of access channels as shown in Fig. 7(b)–(d). We choose communication resources near extreme points as the SFC's extra allocated communication resources c_1. Chosen resources for ES, wind turbine, and PV's SFCs are shown in Table VI.

TABLE VI
COMMUNICATION RESOURCES ALLOCATED TO THREE DISTRIBUTED FREQUENCY REGULATION RESOURCES' SFCS

Communication Resources	ES's SFC	Wind's SFC	PV's SFC
Access Channel $c_1(e^S_{\mathrm{r,b}})$	–	9	9
Base Station $c_1(n^S_{\mathrm{b}})$	120	120	120
Backhaul Link $c_1(e^S_{\mathrm{b,g}})$	–	140	140
Gateway $c_1(n^S_{\mathrm{g}})$	10.5	10.5	10.5

3) Impact of Communication Resources Allocation

In this section, we study impact of communication resources allocation on allocating cost, communication time delay, and SFC's deployment.

3-1) Impact of Communication Resources Allocation on allocating cost: To show effectiveness of our model, we compare it with two other communication resource allocation models. One is greedy node deployment and shortest path deployment (GNSP). The other is greedy node deployment and optimized path deployment (GNOP). The GNSP model first solves the service node's allocation problem by greedily choosing the lowest-cost infrastructure node without considering the cost of the infrastructure link. After selecting infrastructure nodes, the GNSP model then chooses the shortest path between infrastructure nodes as the chosen infrastructure links [28]. The GNOP model is a variant of the GNSP model. Similar to the GNSP model, the GNOP model first chooses the lowest-cost

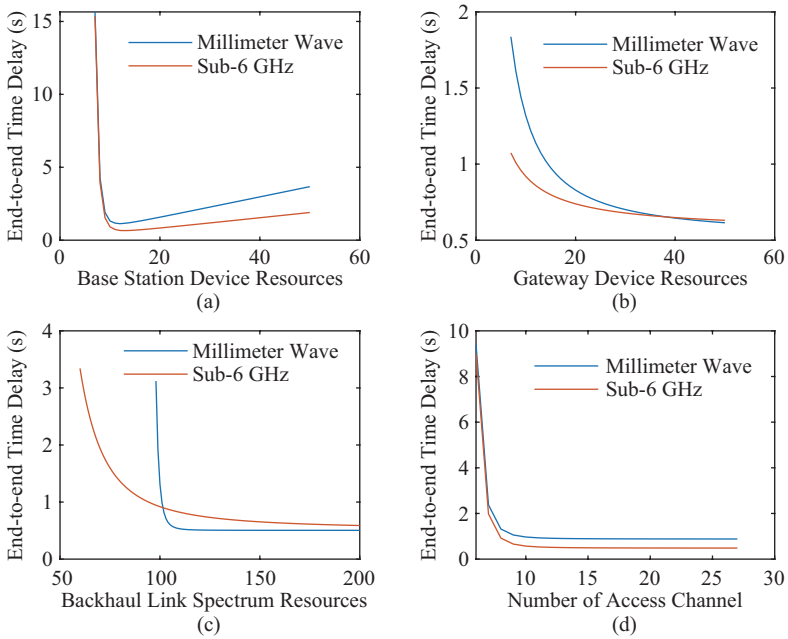

Fig. 7. Impact of four communication resources on end-to-end communication time delay. (a) Base station device resources. (b) Gateway device resources. (c) Backhaul link spectrum resources. (d) The number of access channels.

infrastructure node. After choosing infrastructure nodes, the GNOP model then optimizes infrastructure links' allocating results considering resource allocation constraints, SFC's flow constraints, allocation exclusive constraints, and minimizing allocating cost.

We solve the communication resource allocation problem by solving our proposed model, GNSP model, and GNOP model. We get three different allocating costs and SFCs' deployments, as shown in Table VII and Fig. 8. We can see from Table VII solving our proposed model has lowest allocating cost compared with the GNOP model and GNSP model, which is 1670 p.u. This is because our proposed model coordinately considers node allocation and link allocation problems, which optimizes the SFCs' deployment globally. However, our proposed model has longest computation time, which is 0.58 seconds. Although the GNOP model optimizes service link's allocation problem, its way of solving service node's allocation is heuristic. So, allocating cost of the GNOP model increases by 9.3% compared with our model. Methods of solving service nodes' and service link allocation problems are both heuristic in the GNSP model. So, allocating cost of GNOP model increases by 14.3% compared with our model while the GNOP model has a 0.08 seconds computation time. Computation time of our proposed allocation problem is about 0.58 seconds, which is smaller than time interval of AGC signals' production. We can apply our proposed model to solve the communication resource allocation problem in practice. Besides, as long as the SFCs' resource requirements or communication network's parameters change, problem can be solved again.

TABLE VII
ALLOCATING COST OF THREE MODELS

Model	Allocating Cost	Cost Increase	Computation Time
Our Model	1670 p.u.	–	0.58 s
GNOP	1825 p.u.	9.3%	0.20 s
GNSP	1909 p.u.	14.3%	0.08 s

Figure 8 shows the SFCs' allocating results in three models. We can see ES's SFC and directly connected generators' SFC have the same allocating results in the three models. Allocating results of PV's SFC are the same in the GNSP model and GNOP model, but different in our proposed model. This is because the node resource' capacity price of infrastructure node 12 is cheaper than infrastructure node 11. So, greedy node deployment method will choose infrastructure node 12 instead of infrastructure node 11. Allocating results of wind's SFC are different in the GNSP model, GNOP model, and our proposed model. The chosen infrastructure nodes of the GNSP model and GNOP model are different from those of our proposed model. Besides, chosen infrastructure links of the GNSP model and the GNOP model are different. This is because the GNSP model chooses the shortest infrastructure links while the GNOP model chooses infrastructure links with the lowest cost. Our proposed model shows effectiveness in minimizing allocating cost and deploying frequency regulation resources' SFCs.

3-2) Impact of Communication Resources Allocation on the communication time delay: We calculate communication time delay in extra allocated communication resources case c_1 and compare it with time delay in the base communication resource case c_0 in Table VIII. We can see from Table VIII communication time delay decreases significantly when communication resources increase from base case c_0 to extra allocated case c_1. Time delay of wind turbine $T_{\mathrm{AGC}}^{\mathrm{W}}$ decreases from 919 ms to

TABLE VIII
TIME DELAY OF THREE DISTRIBUTED REGULATION RESOURCES IN BASE AND EXTRA ALLOCATED COMMUNICATION RESOURCES

Delay Type (ms)	$T_{\mathrm{AGC}}^{\mathrm{ES}}$		$T_{\mathrm{AGC}}^{\mathrm{W}}$		$T_{\mathrm{AGC}}^{\mathrm{PV}}$	
	c_1	c_0	c_1	c_0	c_1	c_0
Control Plane T_{con}	–	–	86	471	86	471
User Plane T_{user}	1	1	1	1	1	1
Backhaul T_{bh}	16	19	317	417	77	815
Transmission Network T_{tc}	30	30	30	30	30	30
Total T_{AGC}	47	50	434	919	194	1317

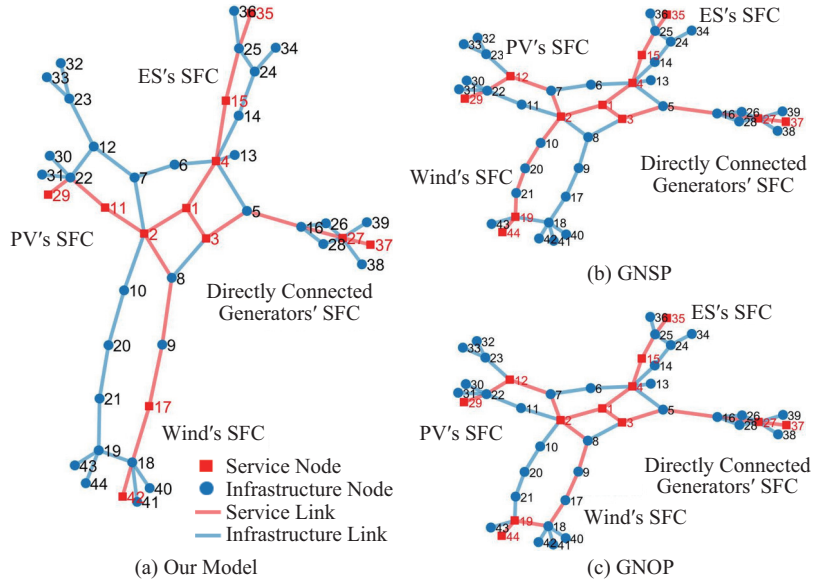

(a) Our Model (b) GNSP (c) GNOP

Fig. 8. Four frequency regulation resources' SFCs allocating results in three models. (a) Our proposed model. (b) GNSP model. (c) GNOP model.

434 ms, and time delay of PV $T_{\mathrm{AGC}}^{\mathrm{PV}}$ decreases from 1317 ms to 194 ms. We perform power system's frequency regulation simulation to show effectiveness of communication resource allocation, and frequency performance indexes are shown in Table IX. Results show CPS-1 increases from 91.2% to 99.6% and the RMSE decreases from 0.0632 to 0.0576 with extra communication resources allocated for AGC's SFC, which are very close to frequency performance of DVRE participating in AGC without delay. Close performance indexes indicate extra communication resources allocated for AGC can help achieve the DVRE's frequency regulation ability.

TABLE IX
FREQUENCY REGULATION PERFORMANCE IN THREE CASES

Case	CPS-1	BAAL	RMSE
1.0% DVRE in AGC with Delay	91.2%	99.4%	0.0632
Extra Communication Resources for AGC	99.6%	99.4%	0.0576
1.0% DVRE in AGC without Delay	100.4%	99.4%	0.0561

3-3) Impact of Communication Resources Allocation on the SFC's deployment: AGC's SFC changes when extra communication resources are allocated. Specifically, nodes' and links' resource capacity requirements increase which may change the SFCs' deployment. We solve communication resource allocation problem in base communication resources case c_0 and extra allocated communication resource case c_1, respectively. We get two different SFCs' deployments, as shown in Fig. 9. Deployment results of ES's SFC and other directly connected generators' SFC are the same since their allocated communication resources in case c_0 and case c_1 are almost the same. However, deployment results of wind's SFC and PV's SFC change because of increase in the SFC's resource requirements. From Fig. 9, we can see infrastructure network chooses different BS nodes, gateway nodes, and backhaul links for wind and PV. The infrastructure network will choose to allocate nodes and links with a higher capacity limit in Fig. 9(b) rather than cheaper nodes and links in Fig. 9(a) to PV's and Wind's SFCs. Allocating cost in Fig. 9(a) is 1620 p.u. while cost in Fig. 9(b) is 2736 p.u. Different allocating results show importance of planning the communication network, which provides a reference for communication network resources allocation.

4) Communication Resources for High VRE Penetrated Power System

Frequency performance drops severely when the VRE penetration is high. In high renewable penetrated power system, communication resources allocation method still works. In this section, we study required time delay and communication resources for DVRE participating in AGC to keep frequency performance at normal level for power systems with different VRE penetration. Normal level is CPS-1 should be larger than 100%, and the BAAL should be larger than 99% according to the North American Electric Reliability (NERC). Results are shown in Table X.

TABLE X
REQUIRED TIME DELAY AND COMMUNICATION RESOURCES CAPACITY UNDER DIFFERENT VRE PENETRATIONS

VRE Penetration	Required Delay (ms)	Access Channel	Base Station	Backhaul Link	Gateway
30%	1135	8	100	100	9.5
35%	926	8	107	100	10.7
40%	678	8	110	102	11
45%	442	8	116	104	11.6
50%	285	9	130	108	13
55%	196	14	170	120	17
60%	131	18	210	150	21
65%	95	25	250	185	25
70%	40	34	550	480	35
75%	35	50	600	550	60
80%	35	50	600	550	60
85%	35	50	600	550	60

We can see from Table X required time delay decreases from 1135 ms to 35 ms when the VRE penetration is from 30% to 85%. Required time delay is 35 ms in power system with VRE penetration above 70%. Power system with VRE penetration

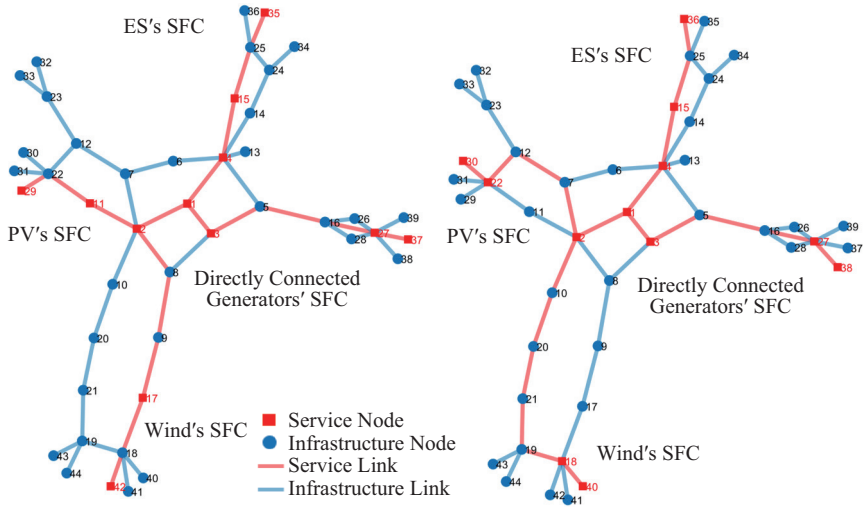

(a) (b)

Fig. 9. Four frequency regulation resources' SFCs allocating results in two communication resources cases. (a) Base communication resources case. (b) Extra allocated communication resources case.

above 70% requires about five times as many communications resources as 30% VRE penetrated power system. Therefore, allocating more communication resources and offering a low-latency communication environment to DVRE can support DVRE's participation in AGC in high VRE penetrated power system.

VII. Conclusion

In this study, we have proposed a communication resources allocation model to reduce time delay in the DVRE's frequency regulation service. We allocate communication devices and wireless spectrum resources to the DVRE's frequency regulation service. Besides, we have analyzed impact of communication resources allocation on the DVRE's frequency regulation in different VRE penetrated HRP-38 systems.

Simulation results allow drawing three conclusions:

1) The communication time delay of DVRE participating in AGC will prevent the DVRE from achieving its ability to provide frequency regulation service. Specifically, when time delay is around 1 second and the VRE penetration is about 30%, DVRE can barely provide frequency regulation service in the HRP-38 system.

2) Allocating more communication resources to DVRE's communication service can decrease communication time delay, which makes DVRE a promising frequency regulation resource.

3) High VRE penetrated power systems require more communication resources than power systems with low VRE penetration. In the HRP-38 system with VRE penetration above 70%, required communication resources are about five times as many as 30% VRE penetrated HRP-38 system to keep frequency performance at the same level.

We will explore impact of other renewable generation on frequency regulation in our future work, such as geothermal power plants and tidal turbines. Besides, we will study performance of DVRE participating in AGC and communication resource allocation in other practical power systems.

References

[1] IRENA, "Global energy transformation: a roadmap to 2050," International Renewable Energy Agency, Abu Dhabi, Apr. 2018.

[2] Z. D. Chu and F. Teng, "Short circuit current constrained UC in high IBG-penetrated power systems," *IEEE Transactions on Power Systems*, vol. 36, no. 4, pp. 3776–3785, Jul. 2021.

[3] K. Peddakapu, M. R. Mohamed, P. Srinivasarao, Y. Arya, P. K. Leung, and D. J. K. Kishore, "A state-of-the-art review on modern and future developments of AGC/LFC of conventional and renewable energy-based power systems," *Renewable Energy Focus*, vol. 43, pp. 146–171, Dec. 2022.

[4] W. L. Zhong, G. Tzounas, and F. Milano, "Improving the power system dynamic response through a combined voltage-frequency control of distributed energy resources," *IEEE Transactions on Power Systems*, vol. 37, no. 6, pp. 4375–4384, Nov. 2022.

[5] M. Cosovic, A. Tsitsimelis, D. Vukobratovic, J. Matamoros, and C. Anton-Haro, "5G mobile cellular networks: Enabling distributed state estimation for smart grids," *IEEE Communications Magazine*, vol. 55, no. 10, pp. 62–69, Oct. 2017.

[6] H. X. Hui, Y. Ding, Q. X. Shi, F. X. Li, Y. H. Song, and J. Y. Yan, "5G network-based internet of things for demand response in smart grid: a survey on application potential," *Applied Energy*, vol. 257, pp. 113972, Jan. 2020.

[7] M. Tao, K. Ota, and M. X. Dong, "Foud: Integrating fog and cloud for 5G-enabled V2G networks," *IEEE Network*, vol. 31, no. 2, pp. 8–13, Mar./Apr. 2017.

[8] Y. Shen, W. Fang, F. Ye, and M. Kadoch, "EV charging behavior analysis using hybrid intelligence for 5G smart grid," *Electronics*, vol. 9, no. 1, pp. 80, Jan. 2020.

[9] F. Malandra and B. Sansò, "A markov-modulated end-to-end delay analysis of large-scale RF mesh networks with time-slotted ALOHA and FHSS for smart grid applications," *IEEE Transactions on Wireless Communications*, vol. 17, no. 11, pp. 7116–7127, Nov. 2018.

[10] Q. Ye, W. H. Zhuang, X. Li, and J. Rao, "End-to-end delay modeling for embedded VNF chains in 5G core networks," *IEEE Internet of Things Journal*, vol. 6, no. 1, pp. 692–704, Feb. 2019.

[11] A. Chilwan and Y. M. Jiang, "Modeling and delay analysis for SDN-based 5G edge clouds," in *2020 IEEE Wireless Communications and Networking Conference (WCNC)*, 2020, pp. 1–7.

[12] N. Aghanoori, M. A. S. Masoum, A. Abu-Siada, and S. Islam, "Enhancement of microgrid operation by considering the cascaded impact of communication delay on system stability and power management," *International Journal of Electrical Power & Energy Systems*, vol. 120, pp. 105964, Sep. 2020.

[13] K. Samarakoon, J. Ekanayake, and N. Jenkins, "Investigation of domestic load control to provide primary frequency response using smart meters," *IEEE Transactions on Smart Grid*, vol. 3, no. 1, pp. 282–292, Mar. 2011.

[14] Y. S. Lin, P. Barooah, S. Meyn, and T. Middelkoop, "Experimental evaluation of frequency regulation from commercial building HVAC systems," *IEEE Transactions on Smart Grid*, vol. 6, no. 2, pp. 776–783, Mar. 2015.

[15] E. Vrettos, E. C. Kara, J. MacDonald, G. Andersson, and D. S. Callaway, "Experimental demonstration of frequency regulation by commercial buildings—part I: modeling and hierarchical control design," *IEEE Transactions on Smart Grid*, vol. 9, no. 4, pp. 3213–3223, Jul. 2018.

[16] H. T. Chien, Y. D. Lin, C. L. Lai, and C. T. Wang, "End-to-end slicing as a service with computing and communication resource allocation for multi-tenant 5G systems," *IEEE Wireless Communications*, vol. 26, no. 5, pp. 104–112, Oct. 2019.

[17] W. L. Wen, Y. Cui, T. Q. S. Quek, F. C. Zheng, and S. Jin, "Joint optimal software caching, computation offloading and communications resource allocation for mobile edge computing," *IEEE Transactions on Vehicular Technology*, vol. 69, no. 7, pp. 7879–7894, Jul. 2020.

[18] X. C. Chen, Y. C. Zhou, L. Yang, and L. Lv, "Hybrid fog/cloud computing resource allocation: Joint consideration of limited communication resources and user credibility," *Computer Communications*, vol. 169, pp. 48–58, Mar. 2021.

[19] L. Liang, H. Ye, G. D. Yu, and G. Y. Li, "Deep-learning-based wireless resource allocation with application to vehicular networks," *Proceedings of the IEEE*, vol. 108, no. 2, pp. 341–356, Feb. 2020.

[20] F. Zhang, Y. Z. Sun, L. Cheng, X. Li, J. H. Chow, and W. X. Zhao, "Measurement and modeling of delays in wide-area closed-loop control systems," *IEEE Transactions on Power Systems*, vol. 30, no. 5, pp. 2426–2433, Sep. 2015.

[21] ITU, "Minimum requirements related to technical performance for IMT-2020 radio interface (S)," ITU, Geneva, Rep. ITU-R M.2410–0, Nov. 2017.

[22] G. Z. Zhang, A. P. Huang, H. G. Shan, J. Wang, T. Q. S. Quek, and Y. D. Yao, "Design and analysis of distributed hopping-based channel access in multi-channel cognitive radio systems with delay constraints," *IEEE Journal on Selected Areas in Communications*, vol. 32, no. 11, pp. 2026–2038, Nov. 2014.

[23] P. Xia, H. S. Jo, and J. G. Andrews, "Fundamentals of inter-cell overhead signaling in heterogeneous cellular networks," *IEEE Journal of Selected Topics in Signal Processing*, vol. 6, no. 3, pp. 257–269, Jun. 2012.

[24] J. G. Andrews, F. Baccelli, and R. K. Ganti, "A tractable approach to coverage and rate in cellular networks," *IEEE Transactions on Communications*, vol. 59, no. 11, pp. 3122–3134, Nov. 2011.

[25] M. R. Akdeniz, Y. P. Liu, M. K. Samimi, S. Sun, S. Rangan, T. S. Rappaport, and E. Erkip, "Millimeter wave channel modeling and cellular capacity evaluation," *IEEE Journal on Selected Areas in Communications*, vol. 32, no. 6, pp. 1164–1179, Jun. 2014.

[26] S. Troia, A. F. R. Vanegas, L. M. M. Zorello, and G. Maier, "Admission control and virtual network embedding in 5G networks: a deep reinforcement-learning approach," *IEEE Access*, vol. 10, pp. 15860–15875, Feb. 2022.

[27] J. Lu and J. Turner, "Efficient mapping of virtual networks onto a shared substrate," Washington University in St. Louis, City of Saint Louis, Tech. WUCSE-2006–35, 2006.

[28] Y. Zhu and M. H. Ammar, "Algorithms for assigning substrate network resources to virtual network components," in *Proceedings IEEE INFOCOM 2006. 25TH IEEE International Conference on Computer Communications*, 2006, pp. 1–12.
[29] M. L. Yu, Y. Yi, J. Rexford, and M. Chiang, "Rethinking virtual network embedding: Substrate support for path splitting and migration," *ACM Sigcomm Computer Communication Review*, vol. 38, no. 2, pp. 17–29, Mar. 2008.
[30] N. M. M. K. Chowdhury, M. R. Rahman, and R. Boutaba, "Virtual network embedding with coordinated node and link mapping," in *IEEE INFOCOM 2009*, 2009, pp. 783–791.
[31] Z. Y. Zhuo, N. Zhang, J. W. Yang, C. Q. Kang, C. Smith, M. J. O'Malley, and B. Kroposki, "Transmission expansion planning test system for AC/DC hybrid grid with high variable renewable energy penetration," *IEEE Transactions on Power Systems*, vol. 35, no. 4, pp. 2597–2608, Jul. 2020.
[32] Z. Y. Zhang, E. S. Du, F. Teng, N. Zhang, and C. Q. Kang, "Modeling frequency dynamics in unit commitment with a high share of renewable energy," *IEEE Transactions on Power Systems*, vol. 35, no. 6, pp. 4383–4395, Nov. 2020.
[33] M. Chowdhury, M. R. Rahman, and R. Boutaba, "ViNEYard: virtual network embedding algorithms with coordinated node and link mapping," *IEEE/ACM Transactions on Networking*, vol. 20, no. 1, pp. 206–219, Feb. 2012.

Hongjie He received a B.S. degree from the Electrical Engineering Department of Huazhong University of Science and Technology, Wuhan, China, in 2018. He is now pursuing his Ph.D. degree at the Electrical Engineering Department of Tsinghua University, Beijing, China. His research interests include power system operation, virtual power plant operation, and power system frequency regulation.

Ning Zhang received both B.S. and Ph.D. degrees from the Electrical Engineering Department of Tsinghua University, Beijing, China, in 2007 and 2012, respectively. He is now an Associate Professor at the same university. His research interests include renewable energy, and power system planning and operation, multiple energy systems integration.

Chongqing Kang received a Ph.D. degree from the Electrical Engineering Department of Tsinghua University in 1997. He is now a Professor at the same university. His research interests include power system planning, power system operation, renewable energy, low carbon electricity technology and load forecasting.

Song Ci received a Ph.D. degree from the University of Nebraska-Lincoln, Lincoln, NE, USA, in 2002. He is currently a Professor of Electrical Engineering with Tsinghua University, Beijing, China. His research interests include large-scale dynamic complex system modeling and optimization, as well as its applications in the areas of Internet and Energy Internet.

Fei Teng received a B.Eng degree in Electrical Engineering from Beihang University, China, in 2009, and M.Sc. and Ph.D. degrees in Electrical Engineering from Imperial College London, U.K., in 2010 and 2015, respectively. Currently, he is a Senior Lecturer in the Department of Electrical and Electronic Engineering, Imperial College London, U.K. His research focuses on cyber-physical modeling, optimization and data analytics of power systems.

Goran Strbac is a Professor of Energy Systems at Imperial College London, London, U.K. He led the development of novel advanced analysis approaches and methodologies that have been extensively used to inform industry, governments, and regulatory bodies about the role and value of emerging new technologies and systems in supporting cost effective evolution to smart low carbon future. He is currently the Director of the joint Imperial-Tsinghua Research Centre on Intelligent Power and Energy Systems, Leading Author in IPCC WG 3, Member of the European Technology and Innovation Platform for Smart Networks for the Energy Transition, and Member of the Joint EU Programme in Energy Systems Integration of the European Energy Research Alliance.